

Seismic cloud of past and present

Kozo Takahashi^{1*}

¹none

Seismic Cloud of Past and Present

[Introduction] Recent observation from the space shows that the prediction from the cloud has been expected to have the success rate of 100%. About one week before S Hyogo Pref. Eq. (1995/01/17 M:7.2), the column of cloud like a small tornado, shown by the attached photo, was observed, and the cloud make us possible to predict the earthquake, because the cloud does not drift but remains at the same point, though the other clouds are drifting with wind. But even though the success rate is high, the alarm rate is low, because the seismic cloud is generated only when the atmosphere is saturated by water vapor, and even if the cloud is generated, it is observed only when it is neither raining nor cloudy.

[Mechanism of generating seismic cloud] Water drops in cumulonimbus change into ice crystals in the area of -10 degs. The melting temperature of the solid is lower on the surface than the inside, and at -10 deg. the crystals are covered with water film. The inside of crystals there are free electrons and positive holes, and the electrons can move to the surface water, but the holes can't, so the water is negatively charged, and the solid part of crystals is positively charged. In the clouds crystals collide with each other. Where lower than -10 deg., the collision approximates to elastic one, and the change of speed of smaller crystals is more significant than that of bigger ones. Then the negative surface water on the smaller crystals moves to the bigger ones, and smaller ones become smaller and positive. On the other hand, the bigger crystals become negative, bigger, and drop down on the ground.

The positive smaller crystals are blown up by an ascending air current. At the cloud top of about 10 km high, the voltage becomes up to about 30 MV. As the conductivity between the cloud top and the ionosphere is not small, and as the potential at the cloud top is much higher than at the ionosphere, so electrons and negative ions flow from the ionosphere into the cloud top, and the ionosphere gets a few MV. This negative current generated by cumulonimbus is compensated by the current between the ionosphere and the ground, which is about 1.8 kA.

The current between the ionosphere and the ground flows, like lightning, along the trace of cosmic ray showers, which is usually invisible, as the resistance in the lower atmosphere is high.

When the seismic cloud was observed before the Eq., the density of Radon (Rn) increased in the spring water and low atmosphere on the source region. This increase makes the conductivity higher locally and tentatively there, and the current increases between the ionosphere and ground. The current density becomes high enough by Pinch Effect to generate the tornado-like cloud, which is similar to the cloud in Wilson cloud chamber. This current is pulsating current, as the cosmic shower changes rapidly in time and space, so the current radiates wide band radio-waves, which are observed as precursory seismic electric fields.

Rn and Radium (Ra) are generated by decay of Uranium (U), and U exists not in the crystal but in the boundary. If micro-cracks run in the source, U, Rn and Ra dissolve into pore water, which mixes in spring water. So, the micro-cracks are essential for the short-term prediction.

[End Remark] Like the seismic cloud, some macroscopic anomalies may become new tools for highly reliable prediction. The observing electric fields, for example, may become to predict the place and magnitude when the source regions are located, much more precisely and reliably than the observing crustal movement which are currently adopted now.

[Reference] Japan Geoscience Union Meeting 2010 S-SS012-08 Mechanism of Generating the Earthquake Cloud just before Shallow Great Earthquakes, Kozo Takahashi

Keywords: seismic cloud, earthquake prediction, short-term prediction, precursory electric fields, locating source regions

Japan Geoscience Union Meeting 2013

(May 19-24 2013 at Makuhari, Chiba, Japan)

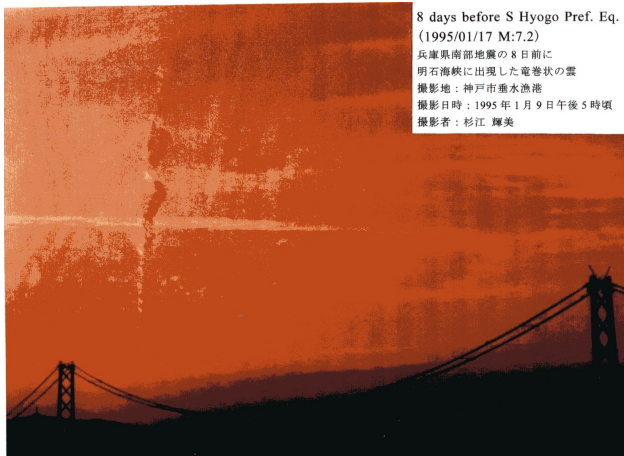
©2013. Japan Geoscience Union. All Rights Reserved.



SSS30-01

Room:106

Time:May 20 16:15-16:30



Numerical simulation to test and evaluate the forecast probabilities by BPT distribution model

Masami Okada^{1*}

¹Meteorological Research Institute, JMA

Numerical simulation was conducted to test and evaluate the performance of Brownian Passage Time (BPT) distribution model on the renewal process which is used by the Earthquake Research Committee of Japan (2001) to compute the probabilities for the forthcoming event in repeating earthquake sequence.

1000 sets consist of N random numbers corresponding to the interevent time following BPT distribution with parameters, the mean of 100 and coefficient of variation of 0.24 were compiled and 1000 random numbers larger than the elapsed time, T_p , since the last event to the forecast were collected from the same BPT population.

The probabilities for relevant event in the forecast period were computed by the BPT distribution model in which the two parameters are determined by the maximum likelihood method from each sequential N data, and they are compared with the hypothetical time interval between the last event and forthcoming one. Log-normal distribution model based on the small sample theory, LN-SST is also used to calculate the probabilities which are compared with those by the BPT distribution model.

In the case of $N=4$, $T_p=75$, and forecast period of 25, the probabilities distribute widely and ones larger than 0.99 appeared abnormally many times. Scores on the mean log-likelihood, MLL and Brier, BS are shown in following table which shows that LN-SST is superior to the BPT distribution model for small sample data.

N	T_p	period	PP	MLL	BS
4	50	25	0.135	-0.585(-0.443)	0.135(0.131)
4	75	25	0.475	-0.969(-0.789)	0.302(0.282)
4	100	40	0.862	-0.867(-0.530)	0.156(0.171)
7	50	25	0.135	-0.476(-0.434)	0.130(0.128)
7	75	25	0.475	-0.755(-0.734)	0.272(0.266)
7	100	40	0.862	-0.611(-0.498)	0.151(0.155)

The N: number of interval data, T_p : elapsed time from the last event to forecast, period: forecast length, and PP: probability calculated from BPT population.

MLL and BS are calculated by the BPT distribution model and those by LN-SST are listed in the parentheses.

Keywords: repeating earthquake, earthquake forecast, BPT distribution, numerical simulation, Bayesian approach, log-normal distribution

Spatiotemporal stability of seismic quiescence 2

Sumio Yoshikawa^{1*}, Naoki Hayashimoto², Tamotsu Aketagawa³

¹Kakioka Magnetic Observatory, ²Meteorological Research Institute, ³Japan Meteorological Agency

In the last meeting of the seismological society of Japan we have reported spatiotemporal stability of the seismic quiescence before the 2011 Tohoku Earthquake. As a result, it became clear that the seismic quiescence had continued to appear stably in the northern part of the source region which became clear around 2001. And also that in some cases the appearance of quiescence area is not directly connected to a large earthquake. This phenomenon is likely to be artificial ones caused by way of parameter setting. We report the results to verify if the behavior of the apparent quiescence is captured by the method of parameter setting.

The method for analysis is the eMAP (Aketagawa and Ito, 2008; Hayashimoto and Aketagawa, 2010), a detection tool of activation and quiescence of seismicity, as it has been used before. It is possible to adjust various kinds of parameters to earthquake detection capability and characteristics of the seismic activity in every area for grasp of spatial pattern of seismicity with this tool.

Seismic quiescence is thought to be caused by a reduction in stress due to localized slip at the contact surface between the fault plane with relatively weak strength. That seismic activity did activated in the southern half, while the quiescence was observed only in the northern half of the focal region in Tohoku Earthquake, seems to reflect that the stress decreased in the northern half, while it increased in the southern half. Although there are cases where apparent quiescence occurs from temporary fluctuation of seismic activity, a most probable seismic quiescence area can be extracted by proper selection of parameters. A possible method for judgment of true seismic quiescence is a so-called doughnut pattern (Mogi, 1969). This phenomenon is thought to be universal to reflect the physical property of the focal region, because the activation area of the seismic activity appears in the asperity where strength is comparatively high in the surrounding of seismic quiescence area.

Keywords: Seismic activity, Quiescence

Dynamic model of hypocenter vibration based on time reversal and prevision of earthquake

Toshiaki Kikuchi^{1*}

¹National Defense Academy

Previously, a hypocenter vibration was analyzed by using time-reversal process for the seismic waves in Suruga Bay. A dynamic model of the hypocenter vibration has proposed from these results. This dynamic model is consistently approved to premonitory symptoms of an earthquake, the main shock, and the aftershock. This model is verified about four earthquakes of M5 or more caused in the vicinity of Mt. Fuji between 2009 and 2012 and the effectiveness is confirmed. The pulse formed at the hypocenter position, that is, time reversal pulse (TRP) was obtained by processing the time reversal to P wave signals received at the observation station in 44 places that enclosed the hypocenter for the earthquake that had occurred in the central part of Suruga Bay in August, 2009. The TRP corresponds to the equivalent sound source that the hypocenter radiates. The clear azimuthal dependency was confirmed to the obtained TRP. To clarify the origin of this azimuthal dependence, the frequency spectrum of the TRP to the azimuth was obtained. The frequency spectrum has changed greatly according to azimuthal. Then, the distribution of the maximum amplitude frequency to azimuthal was obtained. As a result, the maximum amplitude frequency rises greatly as the azimuth changes from west to east and it has descended. The rise of the frequency is due to the movement of the sound source. The moving direction concentrated on the Nishiizunishi station. The head part only of the received signal in the Nishiizunishi St. has expanded though the received signals in Ito and Kawazu St. near the Nishiizunishi St. were usual waveforms.

The point where the beam of narrow angle radiated from the active fault reaches surface of the earth is called a parametric spot, and the head of the pulse to which the head observed here increases is called a parametric head.

The precursor earthquake of M2 or more had occurred 17 times before earthquake of Suruga Bay (2009/8/11). The waveform to accompany the parametric head in that was observed seven times. These parametric heads suggest that the crack begin to move in the active fault by the high-speed. Therefore, it is thought that it is effective to observe the seismic wave of about M2 in a peculiar parametric spot to each active fault, and to examine the change as the prevision of earthquake.

Keywords: Prevision of earthquake, Time reversal, Hypocenter vibration, Seismic wave propagation

Scenario for imminent prediction of strong subduction-zone earthquake via ocean-floor geomagnetic observation network

Yuji Enomoto^{1*}, TABATA, Isao¹

¹Toyama Industrial Technology Center

Ionospheric electron enhancement around the focal region has been observed from about 40 min. before the 2011 Tohoku-Oki earthquake (Heki 2011). On the other hand, ground-level geomagnetic variations prior to the earthquake were as not clear (Minato 2011, Utada et al. 2011). A possible mechanism to explain those electromagnetic anomalies was proposed in terms of coupled interaction of earthquake nucleation with deep Earth gases, where the interaction causes a negatively electrified gas flow due to an exo-electron attachment reaction, as the gases pass through fractured asperities (Enomoto 2012). The pressure-impressed current I in the model is expressed as

$$\log I = 0.5M + \log (5.1 \times 10^2 k e n h^2 D_c / v_i) \quad (1),$$

where e is the electronic charge, n is the density of negatively charged gas molecules, k is a constant of proportionality, M is the earthquake magnitude, h is crack-open gap, v_i is the gas viscosity, D_c is the focal depth. The factor ken could be determined from the laboratory experiments

For earthquake prediction, it is desired to detect clear and identifiable pre-seismic signal. There maybe a possible way to satisfy the condition for subduction-zone earthquake; that is, Fig. 1 showed pre-seismic geomagnetic variation caused by the current estimated from eq.(1) as a function of distance from the epicenter to the geomagnetic observation site with various dip values: the results suggest that clearly identifiable signals attributed to the imminent occurrence of an offshore strong earthquake with a low angle thrust focal mechanism might be observable if geomagnetic measurements are made continuously near the ocean floor epicenter, say within a distance of 20?30 km. Using the observed precursor geomagnetic signals, detected at least three different points on the scenario ocean-floor of subduction-zone earthquake, one could estimate the focal zone (the position of current source), the amount of current, and thus the magnitude. Since both the pre-seismic geomagnetic variation and ionospheric electron enhancement are induced by the same source mechanism, the precursor period might be around several tens minutes as caused by the 2011 Tohoku-Oki earthquake. The net-work observation of geomagnetic fields using submarine cables on the seafloor of scenario subduction-zone earthquake; e.g. the Nankai Trough earthquake, may, therefore, make it possible to predict earthquake occurrence.

References

Enomoto, Y. Couple interaction of earthquake nucleation with deep Earth gases: a possible mechanism for seismo-electromagnetic phenomena, *Geophys. J. Inter.*, 191 (2012) 1210-1214.

Heki, K., 2011. Ionospheric electron enhancement preceding the 2011 Tohhoku-Oki earthquake, *Geophys. Res. Lett.*, 38, L17312?L17316.

Minamoto, Y. et al., 2011. Anomalous variations of geomagnetic intensity possibly induced by the 2011 off the Pacific coast of Toholu earthquake, *Japan Geosci. Union Meeting 2011*, MIS036-P88 (in Japanese).

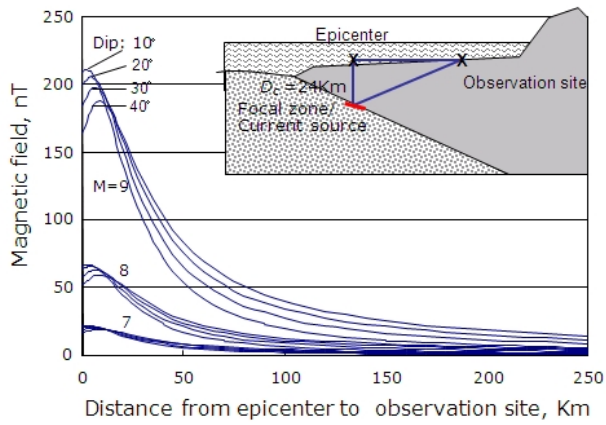
Utada, H. et al., 2011. Geomagnetic field changes in response to the 2011 off the Pacific Coast of Tohoku Earthquake and Tsunami, *Earth planet. Sci. Lett.*, 311, 11?27.

Keywords: Subduction-zone earthquake, Earthquake prediction, Seismo-electromagnetics, Seafloor geomagnetic observation, Exo-electron emission, Fractoemission

SSS30-05

Room:106

Time:May 20 17:15-17:30



On the sea level changes that were witnessed before the 1946 Nankai earthquake on the Pacific coast of Shikoku(2)

Yasuhiro Umeda^{1*}, ITABA, Satoshi¹, HOSO, Yoshinobu²

¹Geological Survey of Japan, AIST, ²DPRI, Kyoto Univ.

Just before the 1946 Nankai earthquake, there are the witness testimonies which the sea level have decreased by 2m~3m at Susaki and Usa bay on the Pacific coast of Shikoku, Japan. To confirm the large amplitude of sea level change before the main shock, the sea level observations were carried out at 7 stations around the Susaki bay from November 2010 to March 2012. The tsunami caused by the 2011 off the Pacific coast of Tohoku earthquake was observed. The tsunami amplitude in Susaki bay has a larger 8 and 20 times than that observed about at 100m (Terada et.al., 2010) and 2300m(JAMSTEC) depth. The spectrum peaks of tsunami are about 85, 50 and 37 minutes. Almost same spectral peaks were observed at the storm and the stable weather. This fact suggests that the same spectra at Susaki are generated by the small vertical movements which occur repeatedly at different sea bottom.

Keywords: Nankai earthquake, sea level change, witness testimony, tsunami

The increase in missing waveform images of the F-net broadband seismograph network preceding the 2011 Tohoku earthquake

Yoshiki SUE^{1*}

¹No institution affiliation

1. Introduction

The F-net is a broadband seismograph network constituted of 73 STS-1 and 2 seismometers. Natural frequency of the seismometers is 120 seconds (STS-2) and longer, thus they can detect long-period ground motion.

On its website, waveform images are provided. The analyses on them so far have shown the following. The Daily Spectral Plot, even on a quiet day, shows existence of vibration with frequency in 2-5 seconds. On days of large fluctuation, the amplitude increases, and the vibrations of 5 seconds and longer are added. The Daily Plot shows fluctuations with the period of several days to 2 weeks, and the Hourly Plot shows those for several hours to several days (Sue, 2010).

2. Analysis

Since seismometers detect ground vibrations, meanwhile their operations might be affected. Thus operational status is investigated. There are two sources on it.

a. Data acquisition trouble log: It is the formal information covering from instantaneous to long-lasting loss of data. Reasons for troubles are shown. While, update of the information is irregular.

b. Missing of waveform images: The website displays the message: "Waveform image is not found". It is surmised that this situation is caused by continuous troubles exceeding 1 day or 1 hour. The reasons are not shown. Update of the information is daily with 2 days delay.

The two sources do not coincide, while overlap partially. At the captioned earthquake, both showed increase before the main shock. Thus analysis on the latter, by counting number of stations with missing images from June 1, 2010 to May 15, 2011, is carried out.

3. Results

As shown in Fig. 1, for 6 months from June 15, 2010 to December 14, 2010, the average number of the stations with missing images = 0.33 with the standard deviation (Sigma) = 1.11 (Notes: For total loss, 10 (1/7 of total) is used for the calculation). It was stable with the daily missing number of less than 1.

There was the first increase from December 22, 2010 to January 18, 2011, and reached the number of 4. Then there was the 2nd increase from February 16, 2011 to March 2, 2011. Especially from February 19 to March 2, it again became 4 stations (Sapporo (Code:HSS), Yamagata (YIG, Iwate pref.), Kesenuma (KSN) and Shiramine (SRN)) as shown in Fig. 2. At the main shock, the number was 2, which was still more than usual. It returned to 0 on May 2. Missing of 4 was 3.3 Sigma, meaning that the state was far from stable. Yamagata and Kesenuma stations are located close to the epicenter, and the distance between them is short. The period of 2nd increase overlapped seismically active period of February 13 to March 2 when M5 earthquakes occurred continuously in the epicentral region.

The data acquisition trouble log shows that "electric power supply trouble" and "data logger restart recording" are the causes of troubles for long and short respectively.

For the Sapporo station, reason of the trouble was "observatory set up", thus the cause might be other than ground motion. In such a case, the missing = 3, meaning 2.4 Sigma. Still it was in a rare state.

4. Discussions

It is assumed that increases of the missing waveform images preceding the big earthquake was because that the F-net could not withstand possible long-period intense vibrations of the earth's surface. For the seismometers, they could be big motions like landslides.

"Electric power supply trouble" might be a good index showing excessive vibration. And rapid increase of "Data logger restart recording" might show the system becoming unstable.

Such phenomena are not observed for the Hi-net seismograph network, probably because of its characteristic (Natural frequency = 1 second).

The author realizes that further studies to increase number of evidences are necessary.

Acknowledgement

SSS30-P01

Room:Convention Hall

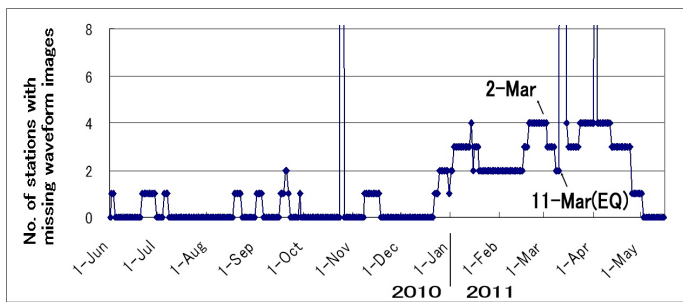
Time:May 20 18:15-19:30

The author thanks NIED for using the data of the F-net.

References

Yoshiki Sue, 2010, Long-period vibration recorded by waveform images of the F-net Broadband Seismograph Network, Part 1, SSJ Fall meeting, D31-12. (In Japanese)

Keywords: F-net, broadband, seismograph network, long period, waveform



HOKKAIDO region			
HIL	DSS	DHG	KMJ
KIP	KSP	NKG	NMR
NOP	SHB	URH	
TOHOKU region			
GLM	HPO	IYG	KSK
KSJ	MMA	TMR	IYS
KANTO region			
BSJ	BSI	HJO	KZS
ONS	OSW	TSK	VMZ
CHUBU region			
ADM	FUJ	IPC	KNM
BYJ	KCK	MMA	SPT
SGJ	SRJ	TIO	WJM
KIBU region			
RSJ	KK	NMT	NOJ
ISA	WTR	YAS	YCA
CHUGOKU region			
MSW	NSK	SAG	DSJ
SHIKOKU region			
ISJ	DAW	HGW	ISA
KIUSU region			
AMM	EJK	SKK	BNJ
KCH	BGM	KYK	SBR
SIR	SHM	HAS	TLO
TKO	TMC	YNG	SMM

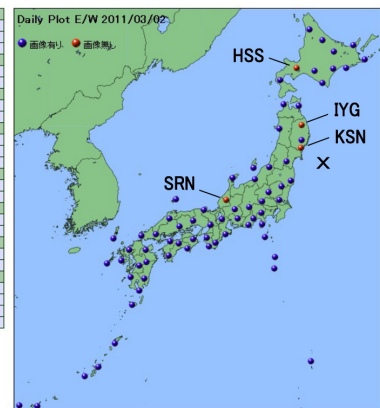


Fig. 1. No. of stations with missing waveform images from June 1, 2010 to May 15, 2011.

Fig. 2. Arrangement of stations with missing waveform images on March 2, 2011 (Source: NIED).

Earthquake prediction from peak gust(8)-Earthquake prediction from cause of earthquake-

Takao Saruwatari^{1*}

¹none

1. Cause of earthquake

It is necessary to verify the hypothesis. It exactly had the doubt in the mantle convection theory that had not been verified yet based on this idea and it searched for the cause of earthquake.

And, it has been understood for the strong wind of a large kinetic energy when the time that becomes an extratropical cyclone from the typhoon and the low-pressure develop, downdraft to collide from a lot of current large earthquakes (After 2000, it is a large earthquake because weather information is necessary) with the earth's crust, and to cause the large earthquake after a while in the collision point.

As for the time lag from the collision to the earthquake generation, it is an artificial earthquake (earthquake that man caused).

(1)The earthquake occurs after storing water begins in a big dam.

(2)The earthquake occurred when a radioactive wastewater was thrown away to underground deep. When abandonment was stopped, it gradually installed.

It is proven. In addition, it was proven dynamically from the wind direction agreement with the axis of the mechanism solution. Moreover, it is thought it is unquestionable by being presumed that the energy of the wind is larger than the energy of the earthquake.

The strong wind of this downdraft can be seen as a dry slot (cloudless area) in the satellite image. It has been understood that the point (Or, it is fundamental) is an epicenter. It is presumed M6.5 or less when there is no dry slot remarkable as for M6.5 or more when there is a remarkable dry slot.

The occurrence time is after for seven months one week later. It is on average after for three months.

The above is announced in the seismology association in October, 2010.

And, it is proven to be able to do the earthquake prediction due to the Tohoku region Pacific Ocean coast earthquake by the above-mentioned method, and announces with JPGU in May, 2011.

<http://www2.jpgu.org/meeting/2011/yokou/MIS036-P85.pdf>

The satellite image chart of 15 o'clock December 3, 2010 and the hypocenter fault chart (From Kyoto University HP) were shown. The tip of the dry slot is corresponding to the source region from those figures, and it is shown that the force of the wind is exactly a cause of earthquake. It is shown to be able to foresee the earthquake occurrence place, the size, and the mechanism solution.

The occurrence of the massive earthquake in Philippine Sea Plate where Nankai Trough is composed is limited in February in August and, in addition, seasonality of abounding is reported in December. This is proof of a lot of coming of a huge typhoon in September, and occurrences of the earthquake in about three months. It is not possible to explain by the mantle convection theory.

The hypothesis with "Energy was liberated when the energy of the swerve accumulated in the plate by the mantle convection exceeded a certain limit and the earthquake occurred" was proven to be a mistake.

2. Recent prediction example

(1)February 18, 2011 low-pressure

M6.4 in east part of Shizuoka Prefecture on March 15, 2011

(2)September 22, 2011 Typhoon No.15 (satellite image at five o'clock)

M6.9 of Sanriku Coast on March 14, 2012.

(3)June 07, 2012 Typhoon No.03 (satellite image at three o'clock)

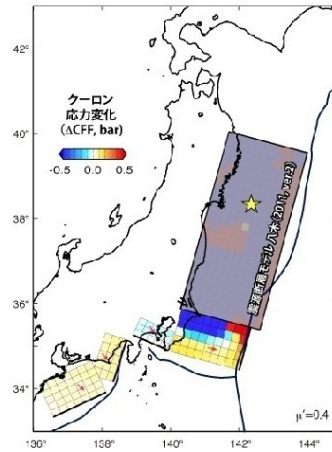
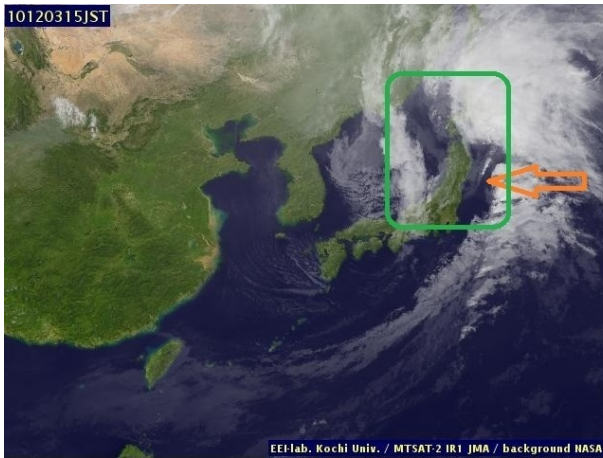
M7.4 of Sanriku Coast on December 07, 2012

Keywords: peak gust, earthquake prediction, dry slot, satellite image, cause of earthquake

SSS30-P02

Room:Convention Hall

Time:May 20 18:15-19:30



A basic theory for earthquake prediction

Tameshige Tsukuda^{1*}

¹Japan Women's Univ.

Earthquakes are generated by the anisotropic principal stress regime in the rock medium. In the preparing process of a large earthquake, the medium would be deformed generating regions of contraction and dilatation around the nucleus of the shearing stresses. A theory for earthquake prediction should be based on an elastic medium model with contraction and dilatation adjacently occurring within and around the seismogenic domain of the medium. The evolution of the medium changes should be monitored in a long time interval: long-, intermediate-, and short-term. The short-term and intermediate-term precursors will be detected when the shearing stress grows as high as the strength of the medium, of which condition we call it a critical state in the preparing process of a large earthquake.

Contraction of the medium should cause high pressures, and dilatation result in low pressures. Such changes in stresses may induce various precursors for an impending large earthquake. The primary precursors are changes of the strain field and micro-seismic activity changes, which are directly related to the elastic changes of the medium. Secondly, migration of fluid within the crust in response to changes of stress level would bring about various precursors. The fluids would transport heat energy, electric charges, and radioactive materials and so on, and, through a preexisting crack network, would incidentally emerge at the ground surface and bring about a variety of precursory phenomena on the ground surface and in the air.

Keywords: earthquake prediction, shearing strain, dilatation, contraction, precursor

Radio wave emission due to rock fracture in various modes and its application to earthquake/volcanic activity detection

Tadashi Takano^{1*}, Jun Kato¹, Yutaro Suzuki¹, Kenji Saegusa¹

¹Nihon University, College of Science and Technology

1. Introduction

Formerly, the microwave emission due to rock fracture was found at the frequency of 300 MHz to 22 GHz [1]. Later, we studied the radio wave emission phenomenon experimentally changing the destruction condition: destruction speed, moisture, and the existence of a thermally shrinkable tube.

This paper describes the measurement system and experimental results. Then, we discuss the availability of the obtained results to the detection of earthquakes and volcanic activities.

2. Measuring system

The measuring system handles 1 MHz-, 300 MHz-, 2GHz-, and 18 GHz-bands. For each frequency band, an antenna, a low noise amplifier and a filter are installed.

We calibrated the measuring system beforehand so that we can estimate the received power from the received waveform height. The 1 MHz receiving system was calibrated as a whole by receiving a broadcasting signal [2]. The phenomenon of a target is instantaneous so that a special recorder and a triggering system to activate a main memory are inevitable.

3. Measured results

In the reference status, a rock is destroyed abruptly in a short time less than 1 sec. The trigger signal was obtained from the highest frequency of 18 GHz with the discrimination level slightly higher than the noise level.

By virtue of this contrivance, the 18 GHz signal was successfully recorded as well as the other frequencies. In the total observation time of 20 msec, signal pulses exist. After expansion, we can see that the radio wave component is included inside the envelope of a pulse shape. There is hardly difference among gabbro, granite, and basalt.

In slow destruction, a rock is destroyed slowly in a long time of several minutes. The obtained waveforms are shown in Fig. 1. In the coarse time scale, we can see a fewer pulses than the reference status. However, more pulses were probably distributed after the recorded time. The pulse height is almost the same as the reference status. The expanded waveform is similar to the case of the reference status.

For destruction with moisture existence, we immersed a rock in water, and then wiped off droplets to use it as an experiment material. There existed hardly a difference from the reference status, but the pulse number is rather increased.

When a rock was destroyed with a thermally shrinkable tube, the signal was received, but weaker than the reference status.

4. Applicability to the detection of earthquakes and volcanic activities

In an earthquake, rock is destroyed around a plate boundary, a fault area, or an asperity. The power of emitted radio wave in a slow destruction was close to the reference status. Therefore, instantaneous power level in an earthquake may be close to the reference status though the average power level is decreased due to a longer destruction time. Accordingly, a sensor to detect radio wave should have an integration capability matched to signal emission circumstance.

A rock is esteemed to coexist with underground water. However, we can obtain the same signal power if the radio wave is generated in the inside of a rock, as indicated experimentally. It was revealed that a radio wave could propagate underground in a gap of several wavelengths [3]. Therefore, a shorter wavelength or a higher frequency is preferred for this application.

5. References

- [1] K. Maki, et al., An experimental study of microwave emission from compression failure of rocks (in Japanese), Jour. of the Seismological Society of Japan, vol.58, no.4, pp.375-384, 2006.
- [2] T. Takano, et al., Radio wave emission from 1 MHz to 18 GHz due to rock fracture and the estimation of the emitted energy (in Japanese), Japan Geoscience Union Meeting, SCG69-P02, Makuhari, May, 2012.
- [3] K. Saegusa, et al., A fundamental study on microwave propagation loss through a ground crack (in Japanese), Trans. of Institute of Electronics, Information and Communication Engineers, Vol.J95-B, No.10, pp. 1364-1371, 2012.

Keywords: Radio wave emission, rock fracture, various modes, earthquake, volcanic activity, detection application

SSS30-P04

Room:Convention Hall

Time:May 20 18:15-19:30

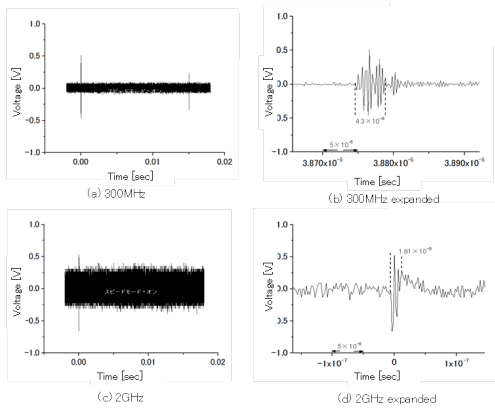


Fig. 1 Measured results in slow destruction of basalt. The trigger signal is from 2GHz channel with a discrimination level of 500 mV. The sampling frequency is 500 MS/s.

Seismicity models of forecasting future M7-class earthquake epicenters in the southern Kanto region, central Japan

Masajiro Imoto^{1*}, Hiroyuki Fujiwara¹, Nobuyuki Morikawa¹, Asako Iwaki¹, Takahiro Maeda¹, Makoto Yamaguchi²

¹NIED, ²NLIRO

The Earthquake Research Committee, Government of Japan, reported that there is a 70% chance of an earthquake with a magnitude of around 7.0 (M7) in southern Kanto in the next 30 years, as estimated based on the past five earthquakes in the region. Probable hypocenters of M7 earthquakes are crucial factors for refining seismic hazard maps for the region.

We take an empirical approach to the problem by deriving probability models of M7 epicenters based on reliable evidence. In the present study, we attempt to employ focal mechanism solutions. First, we calculate the Kagan angle between an observed mechanism and an expected one, which can be estimated by assuming configurations of plate interfaces and relative motions between them. Inter-plate events with Kagan angles below a certain threshold are assigned. We estimate the ratio of the number of inter-plate events to the total number for every 0.1 by 0.1 grid space. After applying smoothing with Akaike's Bayesian information criterion, we obtain statistically significant ratios at every grid. We incorporate this ratio into a model to produce the following different catalogues. 1. Original catalogue of earthquakes exceeding M5.0. 2. Pacific plate earthquakes (Inter-plate and within Pacific plate). 3. Philippine and North American plates. 4. Inter-plate between Philippine and North American plates. 5. Intra-plate (Philippine or North American). We then apply smoothing kernels of different wavelengths to these catalogues and obtain dozens of models.

The likelihood of each model is tested with sixteen past M7 earthquakes. The best model performs 1.3 times better in average probability gain than does the model used in the current national seismic hazard maps for Japan.

Keywords: M7-class earthquakes, Southern Kanto, Earthquake forecasting model, Seismic hazard